Chemical potential of liquids and mixtures via adaptive resolution simulation

Animesh Agarwal, Han Wang, Christof Schütte, and Luigi Delle Site

Citation: The Journal of Chemical Physics **141**, 034102 (2014); doi: 10.1063/1.4886807
View online: http://dx.doi.org/10.1063/1.4886807
View Table of Contents: http://scitation.aip.org/content/aip/journal/jcp/141/3?ver=pdfcov
Published by the AIP Publishing

Chemical potential of liquids and mixtures via adaptive resolution simulation

Animesh Agarwal,[1] Han Wang,[1,a)] Christof Schütte,[2] and Luigi Delle Site[1,b)]
[1]*Institute for Mathematics, Freie Universität, Berlin, Germany*
[2]*Institute for Mathematics, Freie Universität, Berlin, Germany and Zuse Institute Berlin (ZIB), Berlin, Germany*

(Received 17 March 2014; accepted 23 June 2014; published online 16 July 2014)

We employ the adaptive resolution approach AdResS, in its recently developed Grand Canonical-like version (GC-AdResS) [H. Wang, C. Hartmann, C. Schütte, and L. Delle Site, Phys. Rev. X **3**, 011018 (2013)], to calculate the excess chemical potential, μ^{ex}, of various liquids and mixtures. We compare our results with those obtained from full atomistic simulations using the technique of thermodynamic integration and show a satisfactory agreement. In GC-AdResS, the procedure to calculate μ^{ex} corresponds to the process of standard initial equilibration of the system; this implies that, independently of the specific aim of the study, μ^{ex}, for each molecular species, is automatically calculated every time a GC-AdResS simulation is performed. © *2014 AIP Publishing LLC*. [http://dx.doi.org/10.1063/1.4886807]

I. INTRODUCTION

The chemical potential represents an important thermodynamic information for any system, in particular for liquids, where the possibility of combining different substances for forming optimal mixtures is strictly related to knowledge of the chemical potential of each component in the mixture environment. In this perspective, molecular simulation represents a powerful tool for predicting the chemical potential of complex molecular systems. Popular, well established methodologies in Molecular Dynamics (MD) are Widom particle insertion (IPM)[1] and thermodynamic integration (TI).[2] IPM is computationally very demanding often beyond a reasonable limit even in presence of large computational resources, but upon convergence, is rather accurate. TI is computationally convenient but specifically designed to calculate the chemical potential and thus it may not be optimal for employing MD for studying other properties. In fact, TI requires artificial modification of the atomistic interactions (see Appendix A). Recently, we have suggested that the chemical potential could be calculated by employing the Adaptive Resolution Simulation method in its Grand Canonical-like formulation (GC-AdResS).[3–5] AdResS was originally designed to interface regions of space at different levels of molecular resolution within one simulation setup. This allows for large and efficient multiscale simulations where the high resolution region is restricted to a small portion of space and the rest of the system is at coarser level. The recent version of the method, GC-AdResS, given its theoretical framework, should automatically calculate the chemical potential during the process of initial equilibration: in this work, we prove that this is indeed the case and report results for the chemical potential for various liquids and mixtures of particular relevance in (bio)-chemistry and material science. We compare our results with those from full atomistic TI and find a satisfactory agreement. This agreement allows us to conclude that every time a multiscale GC-AdResS is performed, μ^{ex} is automatically calculated for each liquid component and implicitly confirm that the basic thermodynamics of the system is well described by the method. Moreover, in recent work AdResS has been merged with the MARTINI force field.[6,7] In this context, the possibility of checking the consistency of a quantity like the chemical potential can be used as a further argument for the validity of the method in applications to large systems of biological interest. Below we provide the basic technical ingredients of GC-AdResS which are relevant for the calculation of the chemical potential, more specific details can be found in Refs. 4 and 5.

II. FROM ADRESS TO GC-ADRESS

The original idea of AdResS is based on a simple intuitive physical principle:

- Divide the space in three regions, one with atomistic resolution (AT) and one with coarse-grained (spherical) resolution (CG) interfaced by a smaller region with a hybrid treatment, which is usually called transition region or hybrid region.
- Couple the molecules in the different regions through a spatial interpolation formula on the forces

$$\boldsymbol{F}_{i,j} = w(\boldsymbol{r}_i)w(\boldsymbol{r}_j)\boldsymbol{F}^{\mathrm{AT}}_{i,j} + [1 - w(\boldsymbol{r}_i)w(\boldsymbol{r}_j)]\boldsymbol{F}^{\mathrm{CG}}_{i,j}, \tag{1}$$

where i and j indicates two molecules, $\boldsymbol{F}^{\mathrm{AT}}$ is the force derived from the atomistic force field and $\boldsymbol{F}^{\mathrm{CG}}$ from the corresponding coarse-grained potential, $\boldsymbol{r}$ is the center of mass (COM) position of the molecule, and w is an interpolating function which smoothly goes from 0 to 1 (or vice versa) in the transition region (Δ) where the lower resolution is then slowly transformed

a)han.wang@fu-berlin.de
b)dellesite@fu-berlin.de

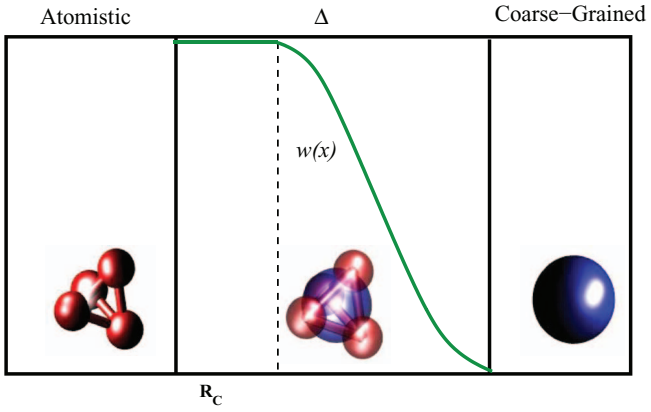

FIG. 1. Pictorial representation of the adaptive box and molecular representation. Here, it is shown the case of the tetrahedral molecule used as a test case in the original development of AdResS. The region on the right, is the low resolution region (coarse-grained), the central part is the transition (hybrid) region Δ, where the switching function $w(x)$ (in green) is defined, and the region on the left, is the high resolution region (atomistic). It must be noticed that differently from the original AdResS, in GC-AdResS the range of definition of $w(x)$ is extended of an amount of $\boldsymbol{R}_c$. The extension of this additional region is equal to the cut-off radius of the atomistic interactions and $w(x)$ takes the constant value of 1. The consequence is that molecules in the atomistic region interact with the rest of the system always and only via well defined atomistic interactions. This characteristic, in turn, allows to write an exact Hamiltonian for the atomistic region and thus treat the system in a Grand-Canonical fashion (see Eq. (12) of Ref. 5).

(according to w) in the high resolution (or vice versa), as illustrated in Fig. 1.

- In the transition region, a thermodynamic force acting on the COM of each molecule and a locally acting thermostat are added to assure the overall thermodynamic equilibrium at a given temperature. The thermodynamic force is defined in such a way that $p_{\mathrm{AT}} + \rho_0 \int_\Delta \boldsymbol{F}_{\mathrm{th}}(\boldsymbol{r}) d\boldsymbol{r} = p_{\mathrm{CG}}$, where p_{AT} is the target pressure of the atomistic system (region), p_{CG} is the pressure of the coarse-grained model, ρ_0 is the target molecular density of the atomistic system (region).[3] An additional locally acting thermostat is added to take care of the loss/gain of energy in the transition region.

In Ref. 5, we have defined necessary conditions in Δ such that the spatial probability distribution of the full-atomistic reference system was reproduced up to a certain (desired) order in the atomistic region of the adaptive system. We have defined the mth order of a spatial (configurational) probability distribution of N molecules, $p(\boldsymbol{r}_1, \ldots, \boldsymbol{r}_N)$, as

$$p^{(m)}(\boldsymbol{r}_1, \ldots, \boldsymbol{r}_m) = \int p(\boldsymbol{r}_1, \ldots, \boldsymbol{r}_m, \boldsymbol{r}_{m+1}, \ldots, \boldsymbol{r}_N)\, d\boldsymbol{r}_{m+1} \ldots d\boldsymbol{r}_N. \quad (2)$$

The first order, often mentioned in this work, corresponds to the molecular number density $\rho(\boldsymbol{r})$. Moreover, we have shown that, because of the necessary conditions, the accuracy in the atomistic region is independent of the accuracy of the coarse-grained model, thus, in the coarse-grained region, one can use a generic liquid of spheres whose only requirement is that it has the same molecular density of the reference system. In the simulation setup, $\boldsymbol{F}_{th}$ is calculated via an iterative procedure using the molecular number density in Δ. The iterative scheme consists of calculating $\boldsymbol{F}_{th}^{k+1}(\boldsymbol{r}) = \boldsymbol{F}_{th}^{k}(\boldsymbol{r}) + \frac{1}{\rho_0^2 \kappa_T} \nabla \rho^k(\boldsymbol{r})$ (κ_T the isothermal compressibility), and the thermodynamic force is considered converged when the target density ρ_0 is reached in Δ. As a result, $\boldsymbol{F}_{th}(\boldsymbol{r})$, acting in Δ, assures that there are no artificial density variations across the system, thus it allows to accurately reproduce the first order of the probability distribution in the atomistic region. Higher orders can be systematically achieved by imposing in Δ a corrective force. For example, the COM-COM radial distribution function correction for the second order.[4] Next, it was proved that indeed the target Grand Canonical distribution, that is the probability distribution of a subsystem (of the size of the atomistic region in GC-AdResS) in a large full atomistic simulation is accurately reproduced. A large number of tests were performed and the reproduction by GC-AdResS of the probability distribution was numerically proved up to (at least) the third order, more than sufficient in MD simulations. Within this framework it was finally shown that the sum of work of $\boldsymbol{F}_{th}(\boldsymbol{r})$ and that of the thermostat corresponds to the difference in chemical potential between the atomistic and coarse-grained resolution; this subject is treated in Sec. III.

III. CALCULATION OF EXCESS CHEMICAL POTENTIAL

In Ref. 5, it has been shown that the chemical potential of the atomistic and coarse-grained resolution are related by the following formula:

$$\mu_{\mathrm{CG}} = \mu_{\mathrm{AT}} + \omega_{\mathrm{th}} + \omega_{\mathrm{Q}}, \quad (3)$$

with μ_{CG} the chemical potential of the coarse-grained system (in GC-AdResS this corresponds to a liquid of generic spheres), μ_{AT} the chemical potential of the atomistic system, $\omega_{\mathrm{th}} = \int_\Delta \boldsymbol{F}_{\mathrm{th}}(\boldsymbol{r}) d\boldsymbol{r}$ the work of the thermodynamic force in the transition region, ω_{Q} the work/heat provided by the thermostat in order to slowly equilibrate the inserted/removed degrees of freedom in the transition region. ω_{Q} is composed by two parts, one, called ω_{extra}, which compensates the dissipation of energy due to the non-conservative interactions in Δ, and another, ω_{DOF}, which is related to the equilibration of the reinserted/removed degrees of freedom (rotational and vibrational). While the determination of ω_{DOF} is not required for our final aim (that is the calculation of the excess chemical potential, as explained later on), the calculation of ω_{extra} is very relevant. However, this calculation is not straightforward and we have proposed to introduce an auxiliary Hamiltonian approach where the coarse-grained and atomistic potential are interpolated, and not the forces as in the original AdResS. Next, we impose that the Hamiltonian system must have the same thermodynamic equilibrium of the original force-based GC-AdResS system; this is done by introducing a thermodynamic force in the auxiliary Hamiltonian approach, which, at the target temperature, keeps the density of particles across the system as in GC-AdResS. In the auxiliary Hamiltonian approach, we have the same equilibrium as the original adaptive (and full atomistic) system and the difference between the work of the original thermodynamic force and the work of the thermodynamic

force calculated in the Hamiltonian approach gives ω_{extra} (further details about this point are given in Appendix B). Moreover, we have proven numerically, for the case of liquid water, that $\omega_{\text{extra}} = \int_\Delta \nabla w(\boldsymbol{r})\langle w(U^{\text{AT}} - U^{\text{CG}})\rangle_{\boldsymbol{r}} d\boldsymbol{r}$, where U_{AT} and U_{CG} are the atomistic and coarse-grained potential. It must be noticed that the auxiliary Hamiltonian approach shall not be considered a Hamiltonian approach to adaptive resolution simulation. In fact, as discussed in Ref. 5 the equilibrium is imposed artificially and *per se* does not have any physical meaning (for more details, see discussion in Appendix B). In Sec. IV of this work, we show analytically that the formula above is exact (at least) at the first order with respect to the probability distribution of the system as defined in Eq. (2). The result above implies that ω_{Q} can be calculated in a straightforward way during the initial equilibration within the standard GC-AdResS code. It must be noticed that, within the AdResS scheme, an approach similar to the auxiliary Hamiltonian has been recently proposed and applied to liquids and mixtures (of toy models so far) by Potestio *et al.*[8,9] (see also Ref. 10 where such an approach is commented). At this point according to (3), if one knows μ_{CG}, then GC-AdResS can automatically provide μ_{AT}. However, we need to do one step more, in fact the quantity of interest is not the total chemical potential, but the excess chemical potential $\mu^{\text{ex}}_{\text{AT}}$ which corresponds to the expression of (3) where the kinetic (ideal gas) part is subtracted. Regarding the kinetic part, one can notice that the contribution coming from the COM is the same for the coarse-grained and for the atomistic molecules, thus it is automatically removed in the calculation of (3). The kinetic part of μ_{AT} due to the rotational and vibrational degrees of freedom corresponds in our case to ω_{DOF} and in principle can be calculated by hand (chemical potential of an isolated molecules). However, such a calculation may become rather tedious for large and/or complex molecules but in our case it is actually not required. In fact, the Gromacs implementation of AdResS considers the removed degrees of freedom as phantom variables but thermally equilibrate them anyway.[11] Thus, the heat provided by the thermostat for the rotational and vibrational part is the same in the atomistic and coarse-graining molecules and is automatically removed in the difference. Finally, the calculation of $\mu^{\text{ex}}_{\text{CG}}$ can be done with standard methods, TI or IPM, which for simple spherical molecules, like those of the coarse-grained system, requires a negligible computational cost. In conclusion, we have the final expression

$$\mu^{\text{ex}}_{\text{AT}} = \mu^{\text{ex}}_{\text{CG}} - \int_\Delta F_{th}(\boldsymbol{r}) d\boldsymbol{r} - \int_\Delta \nabla_{\boldsymbol{r}} w(\boldsymbol{r})\langle w(U^{\text{AT}} - U^{\text{CG}})\rangle_{\boldsymbol{r}} d\boldsymbol{r}. \tag{4}$$

IV. ANALYTIC DERIVATION OF ω_{extra}

In this section, we derive analytically the equivalence: $\omega_{\text{extra}} = \int_\Delta \nabla_{\boldsymbol{r}} w(\boldsymbol{r})\langle w(U^{\text{AT}} - U^{\text{CG}})\rangle_{\boldsymbol{r}} d\boldsymbol{r}$ and define its conceptual limitations. We consider a potential coupling between the atomistic and coarse-grained resolution, that is a spatial interpolation of the atomistic and coarse-grained potential, as done instead for the forces in the standard AdResS

$$U = \sum_{i<j} w(\boldsymbol{r}_i) w(\boldsymbol{r}_j) U^{\text{AT}}_{i,j} + \sum_{i<j} [1 - w(\boldsymbol{r}_i) w(\boldsymbol{r}_j)] U^{\text{CG}}_{i,j}, \tag{5}$$

where $U^{\text{AT}}_{i,j}$ and $U^{\text{CG}}_{i,j}$ are the atomistic and coarse-grained interaction potential between molecule i and j, respectively, defined by

$$U^{\text{AT}}_{i,j} = \sum_{\alpha\in i}\sum_{\beta\in j} U^{\text{AT}}(\boldsymbol{r}_\alpha - \boldsymbol{r}_\beta), \quad U^{\text{CG}}_{i,j} = U^{\text{CG}}(\boldsymbol{r}_i - \boldsymbol{r}_j), \tag{6}$$

where α and β denote the atom indices of the corresponding molecule. The COM of the molecule is defined as

$$\boldsymbol{r}_i = \sum_{\alpha\in i} \frac{m_\alpha}{\sum_{\alpha\in i} m_\alpha} \boldsymbol{r}_\alpha, \tag{7}$$

where m_α is the mass of atom α of molecule i. The potential interpolation (6) provides an auxiliary Hamiltonian to the AdResS system, and the corresponding intermolecular force is given by

$$\begin{aligned}\boldsymbol{F}_{i,j} = {} & w(\boldsymbol{r}_i) w(\boldsymbol{r}_j) \boldsymbol{F}^{\text{AT}}_{i,j} + [1 - w(\boldsymbol{r}_i) w(\boldsymbol{r}_j)] \boldsymbol{F}^{\text{CG}}_{i,j} \\ & - \nabla_{\boldsymbol{r}} w(\boldsymbol{r}_i) w(\boldsymbol{r}_j) \left(U^{\text{AT}}_{i,j} - U^{\text{CG}}_{i,j}\right).\end{aligned} \tag{8}$$

We refer to the AdResS simulation using the potential scheme (8) as auxiliary Hamiltonian AdResS, and all properties of this approach will be added a superscript "H." We define the force of changing representation by

$$\boldsymbol{F}_{\text{rep},i} = \sum_j \nabla_{\boldsymbol{r}} w(\boldsymbol{r}_i) w(\boldsymbol{r}_j) \left(U^{\text{AT}}_{i,j} - U^{\text{CG}}_{i,j}\right). \tag{9}$$

We use the same notation as in our previous work.[5] The thermodynamic variables for the atomistic and coarse-grained regions are denoted by (N_1, V_1, T) and (N_3, V_3, T), respectively. We assume that the transition region is an infinitely thin filter (that is a much smaller region than the atomistic and coarse-grained region) that allows molecules to change resolution as they cross it. Therefore, it is reasonable to assume that

$$V = V_1 + V_3, \tag{10}$$

$$N = N_1 + N_3, \tag{11}$$

where V and N are the total volume and total number of molecules of the system. In this work, we adopt the same assumptions as those listed in Sec. III.C of Ref. 5, i.e., we assume the system to be in the thermodynamic limit, and molecules are short-range correlated (short-ranged must be intended as a range comparable to the size of the transition region). The thermodynamic force for GC-AdResS ($\boldsymbol{F}_{\text{th}}$) and for the auxiliary Hamiltonian AdResS ($\boldsymbol{F}^{\text{H}}_{\text{th}}$), enforce the system to have a flat density

$$\rho_\Delta = \rho_{\text{AT}} = \rho_{\text{CG}} = \rho_0, \tag{12}$$

$$\rho^{\text{H}}_\Delta = \rho_{\text{AT}} = \rho_{\text{CG}} = \rho_0, \tag{13}$$

where ρ_0 is the equilibrium number density of the system defined by $\rho_0 = N/V$. As shown in Refs. 3 and 5, $\boldsymbol{F}_{\text{th}}$ provides the balance of the grand potential or equivalently

$$p_{\text{AT}} = p_{\text{CG}} - \rho_0\, \omega_{\text{th}}, \tag{14}$$

where ω_{th} denotes the work of the thermodynamic force $\boldsymbol{F}_{\text{th}}$.

Instead, when we consider the auxiliary Hamiltonian approach, the third term on the R.H.S. of Eq. (8) is not symmetric with respect to molecules i and j, therefore, the Newton's

action-reaction law (momentum conservation) does not hold anymore. As a consequence, the pressure relation between the AT and CG resolution (14) does not hold and should be derived again. Now assume, for simplicity and without lost of generality, that the system changes resolution only along the x direction. We impose an infinitesimal increment of the volume ΔV to the AT region, and apply the same decrement of the volume $-\Delta V$ to the CG region. The volume of the transition region is kept constant as if it is an ideal "piston" that moves toward the CG region by an amount ΔL. We assume $\Delta V = \Delta L \cdot S$, where S is the cutting surface area. The displacement ΔL should be infinitesimal, i.e., much smaller than the size of the transition region. This is achievable by taking the limit of $\Delta L \to 0$, while keeping the system size fixed. It must also be noticed that the displacements of the molecules are infinitesimal, so it can be reasonably assumed that the resolution of the molecules remains the same under a displacement of ΔL. Therefore, the change of the free energy of the system is approximately

$$\begin{aligned}\Delta A \approx\ & A_{\mathrm{AT}}(N_1, V_1 + \Delta V, T) - A_{\mathrm{AT}}(N_1, V_1, T) \\ & + A_{\mathrm{CG}}(N_3, V_3 - \Delta V, T) - A_{\mathrm{CG}}(N_3, V_3, T) \\ & - \int_{\Delta_x} dx\, \rho_0 S\, \Delta L \cdot \left[\boldsymbol{F}^{\mathrm{H}}_{\mathrm{th}}(x) - \langle \boldsymbol{F}_{\mathrm{rep}}(x)\rangle\right], \end{aligned} \tag{15}$$

where A_{AT} and A_{CG} are the free energies of the AT and CG region, respectively. Δx is the linear dimension of the transition region along x. Since the resolution changes only along x, the two one-particle forces depend only on x, and only have the component along x. This can be easily generalized to changing resolution in any direction, i.e., properly replacing x by $\boldsymbol{r}$. The expression of Eq. (15) as a sum of different terms is justified by the hypothesis of treating the system in the thermodynamic limit, and by the hypothesis that the interactions are short-ranged compared to the size of the transition region. N_1 and N_3 are the numbers of molecules in the AT and CG region, and V_1 and V_3 are the volume in the AT and CG region, respectively; T is the temperature of the system. The last term is originated by the work done by the ideal piston. This term is composed by two parts, the first corresponding to the work done by the thermodynamic force, and the second corresponding to the work done by the force of changing representation (which does not vanish due to the violation of the Newton's action-reaction law). The first and second term of Eq. (8) being forces based on pairwise interactions only, do not contribute to the difference of energy; in fact their total work is zero (as long as the transition region moves infinitesimally along x). The notation $\langle\cdot\rangle$ in Eq. (15) denotes the ensemble average, which will be specified soon. It is straightforward to show that

$$\Delta A \approx -p_{\mathrm{AT}} \Delta V + p_{\mathrm{CG}} \Delta V - \rho_0 \Delta V \left(\omega^{\mathrm{H}}_{\mathrm{th}} - \omega_{\mathrm{rep}}\right), \tag{16}$$

where $\omega^{\mathrm{H}}_{\mathrm{th}}$ is the work of the thermodynamic force $\boldsymbol{F}^{\mathrm{H}}_{\mathrm{th}}$, and ω_{rep} is the work of changing representation, which can be explicitly written down in a general form as

$$\begin{aligned}\omega_{\mathrm{rep}} &= \int_{\Delta} d\boldsymbol{r}\, \langle \boldsymbol{F}_{\mathrm{rep}}(\boldsymbol{r})\rangle \\ &= \int_{\Delta} d\boldsymbol{r}\, \nabla_{\boldsymbol{r}} w(\boldsymbol{r}) \Big\langle w(\boldsymbol{r}') \Big[\sum_{\alpha,\beta} U^{\mathrm{AT}}(\boldsymbol{r}_\alpha - \boldsymbol{r}'_\beta) \\ &\quad - U^{\mathrm{CG}}(\boldsymbol{r} - \boldsymbol{r}') \Big] \Big\rangle_{\boldsymbol{r}';\boldsymbol{r}}. \end{aligned} \tag{17}$$

The average is performed over all possible positions of the second molecule (i.e., $\boldsymbol{r}'$), at fixed position of the first molecule (i.e., $\boldsymbol{r}$) in the pairwise interaction. In case of molecules containing more than one atom, the average is also made over all possible conformations in the atomistic resolution. In the thermodynamic limit, the equilibrium volume of the AT region maximizes the free energy, i.e., $\Delta A/\Delta V = 0$, which yields

$$p_{\mathrm{CG}} - p_{\mathrm{AT}} = \rho_0 \left(\omega^{\mathrm{H}}_{\mathrm{th}} - \omega_{\mathrm{rep}}\right). \tag{18}$$

Comparing the expression above with that obtained for GC-AdResS (Eq. (14)), we have

$$\omega_{\mathrm{rep}} = \omega^{\mathrm{H}}_{\mathrm{th}} - \omega_{\mathrm{th}}, \tag{19}$$

which relates the thermodynamic force of the auxiliary Hamiltonian AdResS and the GC-AdResS.

In Ref. 5, we proved that under proper assumptions, when the flat density profile is enforced by the thermodynamic force, the chemical potential difference between the different resolutions is given by

$$\mu_{\mathrm{CG}} - \mu_{\mathrm{AT}} = \omega_{\mathrm{th}} + \omega_{\mathrm{DOF}} + \omega_{\mathrm{extra}}. \tag{20}$$

The same argument can be applied to the auxiliary Hamiltonian approach, and yields the chemical potential difference between the AT and CG resolutions

$$\mu_{\mathrm{CG}} - \mu_{\mathrm{AT}} = \omega^{\mathrm{H}}_{\mathrm{th}} + \omega_{\mathrm{DOF}}. \tag{21}$$

In the auxiliary Hamiltonian, we do not have the term ω_{extra} in the above formula (being the term ω_{extra} in GC-AdResS, generated by the non-conservative effect of the force interpolation). By comparing (20) with (21), we have the relation

$$\omega_{\mathrm{extra}} = \omega^{\mathrm{H}}_{\mathrm{th}} - \omega_{\mathrm{th}}, \tag{22}$$

which also relates the thermodynamic force of the auxiliary Hamiltonian AdResS and GC-AdResS.

From Eqs. (19) and (22), we find the extra work of the thermostat in GC-AdResS being identical to the work of changing representation of the auxiliary Hamiltonian approach

$$\omega_{\mathrm{extra}} = \omega_{\mathrm{rep}}, \tag{23}$$

which basically proves the statement at the beginning of this section. The ensemble average on the R.H.S. of Eq. (17) is performed in the ensemble of the system treated with the potential interpolation approach, and the question is if the ensemble average is equivalent if it is performed in the simulation where the force interpolation approach is used. It is obvious that the spatial probability distribution corresponding to

the system treated with the potential interpolation is consistent with the force interpolation at least up to the first order. It is also possible to systematically obtain equivalence in the ensemble average operation at higher orders of accuracy of the probability distribution, as, for example, it is done for the radial distribution function in Ref. 4. However, here we do not consider higher order corrections, because it has been numerically shown that actually the ensemble average of $\boldsymbol{F}_{\text{rep}}$ does not depend on in which ensemble it is calculated.[5] Therefore, we use Eq. (23) to calculate ω_{extra}, and measure the ensemble average by the standard AdResS. As previously discussed, in the Gromacs implementation, the CG molecules also keep the atomistic degrees of freedom even though they are in the CG region, therefore, the kinetic part of μ_{AT} and μ_{CG} are identical, and ω_{DOF} vanishes. Therefore, by inserting Eq. (23) into (20), we have

$$\mu_{\text{AT}}^{\text{ex}} = \mu_{\text{CG}}^{\text{ex}} - \int_{\Delta} d\boldsymbol{r}\, \boldsymbol{F}_{\text{th}}(\boldsymbol{r}) - \int_{\Delta} d\boldsymbol{r}\, \nabla_{\boldsymbol{r}} w(\boldsymbol{r}) \times \left\langle w(\boldsymbol{r}') \left[\sum_{\alpha,\beta} U^{\text{AT}}(\boldsymbol{r}_{\alpha} - \boldsymbol{r}'_{\beta}) - U^{\text{CG}}(\boldsymbol{r} - \boldsymbol{r}') \right] \right\rangle_{\boldsymbol{r}';\boldsymbol{r}}. \tag{24}$$

The extension of Eq. (24) to multicomponent systems is reported in Appendix C, while in Sec. V we apply the method to the calculation of μ^{ex} to liquids and mixtures.

V. RESULTS AND DISCUSSION

We have calculated μ^{ex} for different liquids and mixtures, choosing cases which are representative of a large class of systems. Hydrophobic solvation in methane/water and in ethane/water mixtures, hydrophilic solvation in urea/water, a balance of both in water/tert-Butyl alcohol (TBA) mixture, other liquids, e.g., pure methanol and DMSO (and their mixtures with water), non-aqueous mixtures in TBA/DMSO and alkane liquids such as methane, ethane, and propane. Moreover, systems as water/urea are commonly used as cosolvent of biological molecules[12] while systems as tert-Butyl alcohol/water play a key role in modern technology,[13] thus they are of high interest *per se*. All technical details of each simulation are presented in Appendix A.

Results are reported in Table I, where the comparison with values obtained using full atomistic TI and available experiments, at the same concentrations, of our calculation is made; in our previous work we have already shown that value of the chemical potential of liquid water obtained with IPM is well reproduced by GC-AdResS, however the computational cost of IMP was very large, thus we do not consider calculations done with IPM in this paper. The agreement with full atomistic TI simulations is satisfactory in all cases, and thus it proves the solidity of GC-AdResS in describing the essential thermodynamics of a large class of systems. We also compare the obtained values with those available in literature.[15,18] Although the concentration of the minor component in the mixtures that we consider, is higher than the concentrations considered in Refs. 15 and 18, we are anyway in the very dilute regime and thus the chemical potential should not change in a significant way; we have verified such a supposed consistency for one relevant system (see discussion about Fig. 3). The chemical potential of kth liquid's component in a mixture is calculated as (see Appendix C)

$$\mu_{\text{AT}}^{\text{ex},k} = \mu_{\text{CG}}^{\text{ex},k} - \int_{\Delta} \boldsymbol{F}_{\text{th}}^{k}(\boldsymbol{r}) d\boldsymbol{r} - \int_{\Delta} \nabla_{\boldsymbol{r}} w(\boldsymbol{r}) \langle w(U^{\text{AT}} - U^{\text{CG}}) \rangle_{\boldsymbol{r},k} d\boldsymbol{r}, \tag{25}$$

TABLE I. The excess chemical potential of different liquids and mixtures in kJ/mol calculated from GC-AdResS and TI of full atomistic simulations. Experimental values for systems at the same concentrations used in simulation are also reported for comparison. For pure systems (water and methanol), we compare our values with those obtained in literature using the same force field and computational code. For mixtures, most of the values from literature (simulation and experiments) are available at lower concentrations (see Refs. 15 and 18). However, since we are always in a very dilute regime the chemical potential does not change significantly. We have provided evidence for the TBA/water mixture that such consistency holds (see Fig. 3). Note that the chemical potential of water in dilute mixtures is the same of pure water and is not reported above.

Liquid component	Mole fraction of solute	GC-AdResS	TI	Experiment
Water	…	− 22.8 ± 0.2	− 22.1 ± 0.3	− 23.5[14]
Methane	…	− 4.6 ± 0.1	− 5.2 ± 0.1	…
Ethane	…	− 8.2 ± 0.3	− 8.8 ± 0.1	…
Propane	…	− 8.5 ± 0.1	− 9.5 ± 0.2	…
Methanol	…	− 20.1 ± 0.1	− 20.6 ± 0.4	− 20.5[15]
DMSO	…	− 32.2 ± 0.3	− 34.7 ± 0.7	− 32.2[16]
Methanol in methanol/water mixture	0.01	− 18.1 ± 0.2	− 19.7 ± 0.2	…
Methane in methane/water mixture	0.006	9.1 ± 0.1	8.5 ± 0.2	…
Urea in urea/water mixture	0.02	− 56.1 ± 0.6	− 58.2 ± 0.5	− 57.8 ± 2.5[17]
Ethane in ethane/water mixture	0.006	7.2 ± 0.2	7.4 ± 0.3	…
TBA in water/TBA mixture	0.001	− 19.5 ± 0.3	− 20.8 ± 0.6	− 19.0[18]
DMSO in DMSO/water mixture	0.01	− 31.4 ± 0.5	− 33.2 ± 0.3	…
TBA in TBA/DMSO mixture	0.02	− 24.8 ± 0.4	− 24.0 ± 0.5	…

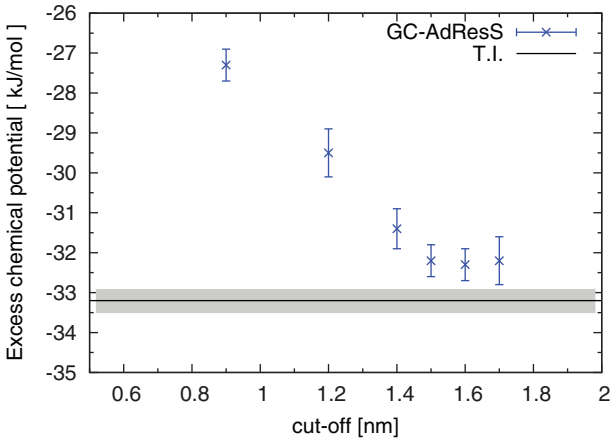

FIG. 2. Excess chemical potential of Dimethyl sulfoxide (DMSO) in water as a function of cut-off radius calculated using GC-AdResS. The value obtained from thermodynamic integration calculation in also shown, with a gray region indicating the standard deviation. This value was calculated using a cut-off radius of 1.4 nm. It was seen that the value does not change significantly if the cut-off radius is varied.

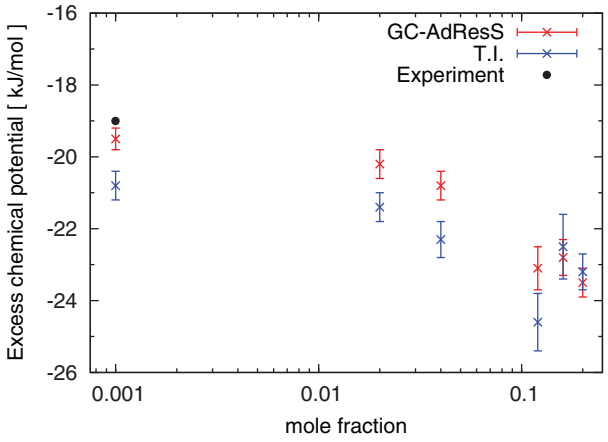

FIG. 3. Excess chemical potential of tert-butyl alcohol (TBA) in water for different concentrations (in logarithmic scale), calculated using GC-AdResS. The results are compared with thermodynamic integration values. At mole-fraction $x_{\mathrm{TBA}} = 0.001$, the experiment value is shown.

where $\boldsymbol{F}^k_{\mathrm{th}}(x)$ is the thermodynamic force applied to the molecules of the kth component; this assures that, at the given concentration, the density of molecules of species k, in the transition region, is equivalent to the density of the same liquid's component in a reference full atomistic simulation. The ensemble average is taken over the position of the second molecule, provided that the first molecule is of species k, and located at position $\boldsymbol{r}$.

A complementary information to Table I are Figs. 2 and 3. In Fig. 2, we have studied the behavior of μ^{ex} as a function of the interaction cutoff. In fact, the current version of GC-AdResS, employs the reaction field method for treating electrostatic interactions in the atomistic region, and the cut-off is likely to play a role in some of the systems investigated. Fig. 2, for the case of DMSO/water mixture, confirms our intuition and suggests that we could systematically improve the accuracy by increasing the cutoff, and at a value of about 1.5 nm, μ^{ex} converges. In any case, at a value of 1.4 nm, which is the one routinely used in full atomistic simulations and used by us, the value obtained with GC-AdResS is already satisfactory. The cut-off radii used for other systems are reported in Appendix A. A further question that may arise is the capability of our method to predict the behavior of μ^{ex} as a function of the concentration, above all in the very dilute regime. In Fig. 3, we have performed such a study for the case of TBA/water mixture, we show a good agreement between GC-AdResS and TI and show that at a very dilute concentration our calculated value is close to that of experiments, moreover the trend, regarding the TI calculations, is consistent with that reported in Ref. 18.

In essence, according to the results obtained, GC-AdResS allows an on-the-fly determination of μ^{ex} of each component of a liquid, whenever a simulation is performed, without extra computational costs. Moreover, Fig. 4 shows the action of the thermodynamic force and of the thermostat in the transition region Δ for TBA-water; the molecular density is sufficiently close to that of reference (the largest difference is below 20% and the average difference is below 10%), and thus it assures that in the atomistic region there are no (significant) artificial effects on the molecular density due to the perturbation represented by the interpolation of forces in Δ.

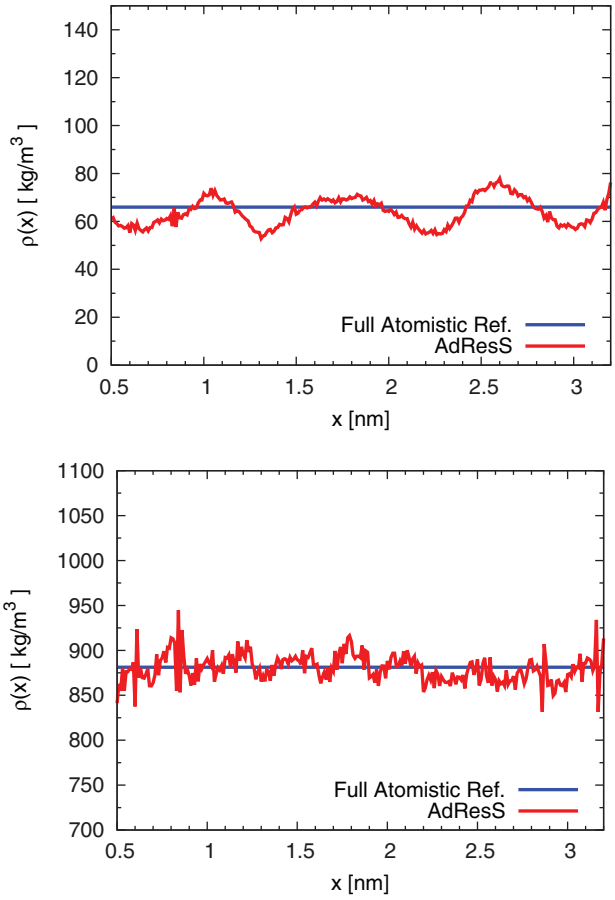

FIG. 4. Top: Molecular density profile in Δ for TBA/water mixture; bottom, the same plot for water. Among all the systems considered, in this case the action of the thermodynamic force and that of the thermostat leads to the largest deviation from the reference all atomistic average density; however, even in this case the discrepancy is negligible. The mole-fraction is $x_{\mathrm{TBA}} = 0.02$, and the cut-off radius is 0.9 nm.

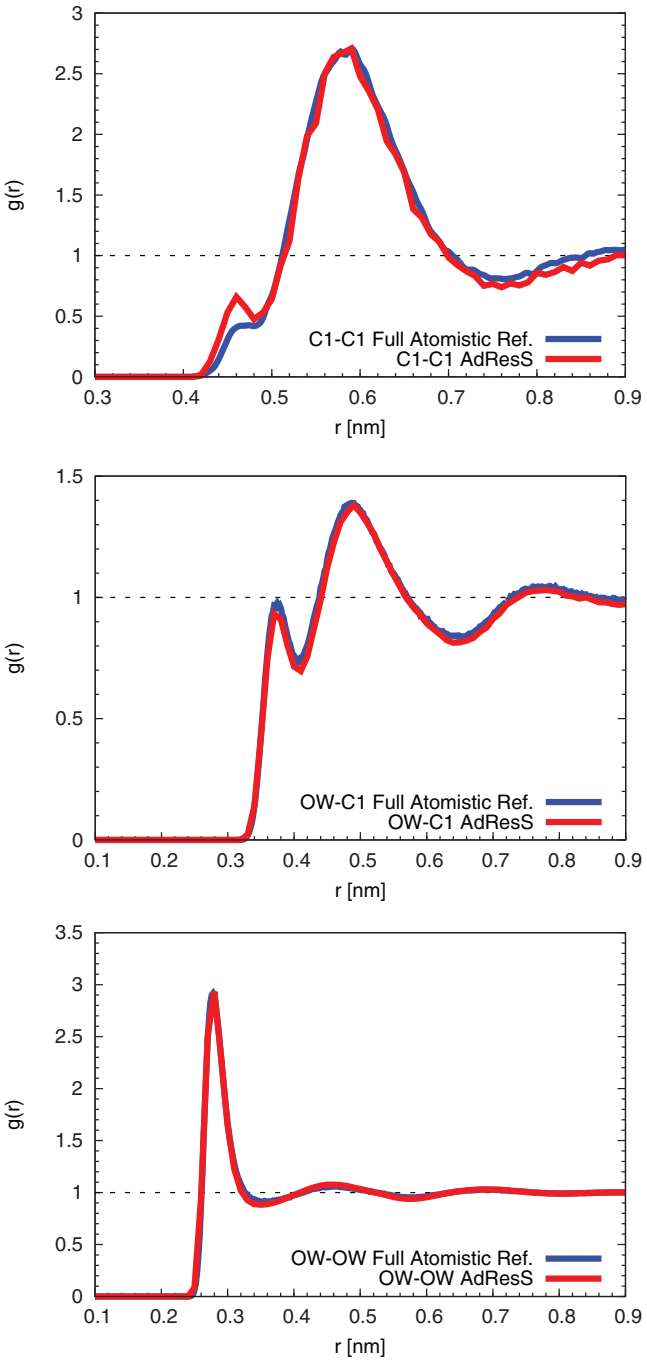

FIG. 5. Top: TBA-TBA radial distribution function; middle: the same plot for TBA-water; bottom: for water-water. Red: the results of the AdResS simulation. The $g(r)$ is calculated only in the atomistic region. Blue: the results of a full-atomistic reference simulation that has the same simulation region as AdResS. The mole-fraction is $x_{\mathrm{TBA}} = 0.02$, and the cut-off radius is 0.9 nm.

In Fig. 5, we report various radial distribution functions for TBA-water in the atomistic region of the adaptive setup. The agreement with data from a full atomistic simulation is highly satisfactory. Moreover, it must be underlined that, on purpose, we have chosen extreme technical conditions, that is, a very small atomistic and coarse-grained region (0.5 nm) and a relatively large transition region (2.7 nm). Even in these conditions we prove that local properties as those of Figs. 4 and 5, together with a relevant thermodynamics quantity as μ^{ex} are well reproduced. This example shows the key features of GC-AdResS, that is, a multiscale simulation where the chemical potential of each component is obtained without extra computational costs and with high accuracy in a simulation where other properties are also calculated with high accuracy. It must also be noticed that the system corresponding to the figures is, among all the system considered, the case where the action of the thermodynamic force and of the thermostat produces the less accurate agreement with the reference data.

VI. EFFICIENCY

In order to show the numerical efficiency of our approach, we compare the time taken to do a full GC-AdResS simulation and the time for a thermodynamic integration calculation for different systems with varied concentration of TBA in water. The total time required for a GC-AdResS simulation consists of the time taken to obtain a converged thermodynamic force and the time taken to obtain the coarse-grained chemical potential. The time taken to complete TI procedure at each value of λ is summed up to obtain the total time. In this work, the TI is done in two stages, first the van der Waals interactions are coupled followed by the electrostatic coupling. At each stage, 21 equally distributed values of λ are used, therefore, in total 42 simulations were performed to calculate each TI chemical potential value. In an AdResS simulation, the initial guess of the thermodynamic force largely determines the time for convergence. We started with a randomly chosen initial guess (-42 kJ/mol, we picked a small value because the TBA molecule is hydrophilic) for system with the highest mole fraction of TBA. For all the other systems, we used the converged thermodynamic force obtained from the first system as an initial guess. The convergence was much faster in all the other cases using this approach. Table II shows the number of iterations required for the thermodynamic force convergence in GC-AdResS and total time required for GC-AdResS and TI calculation. The advantage of GC-AdResS over TI is that we get two values of excess chemical potential for both solute and solvent in a single calculation, while in TI, the whole process has to be repeated to get the excess chemical potential of the other component. For very dilute systems ($x_{\mathrm{TBA}} = 0.001$), however, one has to take a very large systems in GC-AdResS (see Appendix A for system size). It

TABLE II. Time required for a full GC-AdResS and thermodynamic integration (TI) calculation for tert-butyl-alcohol (TBA) in water at different mole-fractions. The "*" means that a larger system was used for the very dilute system ($x_{\mathrm{TBA}} = 0.001$), see Appendix A for details. All the simulations were performed on a workstation that has two Quad-Core AMD Opteron(tm) 2376 Processors.

	GC-AdResS		TI
x_{TBA}	No. of iterations	Time (h)	Time (h)
0.200	20	52.4	30.8
0.160	5	15.1	31.0
0.120	5	16.3	29.9
0.040	8	27.2	26.7
0.020	8	28.8	26.6
0.001*	20	252	202

takes a large amount of time for the thermodynamic force to reach convergence, and hence TI is always a better option at such low concentrations with a much smaller system size at the same mole fraction.

VII. CURRENT COMPUTATIONAL CONVENIENCE: A CRITICAL APPRAISAL

The natural question arising from the discussion above is whether or not GC-AdResS is a more convenient technical tool for calculating μ^{ex} compared to TI. Currently, the answer is neither negative nor positive, although the current work is the first step toward a potentially positive answer for the future. In fact, the fastest version of AdResS is implemented in the GROMACS code;[20] using the Gromacs version 4.5.1 a speedup of a factor four with respect to full atomistic simulations has been reported for aqueous mixtures.[12,19] In this case, GC-AdResS was more convenient than TI because in one simulation one could obtain the chemical potential of each liquid component and at the same time calculate structural properties (e.g., radial distribution functions). However, in the successive version of GROMACS 4.6.1 the performance of atomistic simulations (above all of SPC/E water) has been highly improved while the corresponding implementation of AdResS is not optimized yet. At the current state, AdResS can only assure a speed up factor between 2 and 3 for large systems (30 000 molecules) compared to full atomistic simulations (except for pure SPC/E water systems). As a consequence for the calculation of μ^{ex}, TI is in general computationally less demanding than AdResS . Another point that must be considered (in perspective) for a fair comparison between TI and GC-AdResS, is the following: even if AdResS is optimized, in any code, TI has the advantage that one can use one single molecule in the simulation box to mimic the minor component of a mixture. In our case, instead, we must treat, technically speaking, a true mixture with a certain number of molecules of the minor component immersed in the liquid of the major component. Thus, at low concentrations, GC-AdResS simulations require larger systems than those required by TI, moreover, because of the low density of the minor component, the convergence of the corresponding thermodynamic force requires long simulations. Thus, for very dilute systems, if one is interested only in the chemical potential, TI shall be preferred to GC-AdResS, however, if the interest goes beyond the calculation of the chemical potential (e.g., radial distribution functions), then (optimized) GC-AdResS would still be more convenient. When the concentration becomes higher, GC-AdResS may become preferable for both tasks: general properties of the mixture and chemical potential, not only because in this case one requires larger systems, but also because the convergence of the thermodynamic force of the minor component is much faster. Moreover, we would have the flexibility of calculating the chemical potential of both components in one simulation run, whereas in TI, one needs to run two separate simulations in order to get the chemical potential of both components. The results reported in Sec. VI about the current efficiency of GC-AdResS are rather encouraging, however currently there is not a clear convenience in using GC-AdResS instead of TI for calculating μ^{ex}; in any case the technical aspects of code optimization must be reported and we must make clear that the aim of this work is to show that the automatic calculation of μ^{ex}, independently from the simulation code in which is implemented and its computational cost, is a "conceptual" feature of GC-AdResS.

VIII. CONCLUSION

We have shown the accuracy of GC-AdResS in calculating the excess chemical potential for a representative class of complex liquids and mixtures. For any system, the initial equilibration process, that is the determination of the thermodynamic force, automatically delivers the chemical potential. The only additional calculation required is that of μ^{ex}_{CG} which implies the use of IPM or TI, but for a liquid of simple spheres, thus computationally negligible. The essential message is that GC-AdResS would be, *per se*, a reliable multiscale technique to calculate the chemical potential and, in perspective, upon computational/technical optimization it may become an efficient tool for calculating μ^{ex} compared to current techniques in MD such as TI.

ACKNOWLEDGMENTS

This work was supported by the Deutsche Forschungsgemeinschaft (DFG) with the Heisenberg grant provided to L.D.S (Grant code DE 1140/5-1) and with its associate DFG grants for A.G. (Grant code DE 1140/7-1) and for H.W. (Grant code DE 1140/4-2). H.W. and C.S. thank the financial support by DFG research center MATHEON. We thank Christoph Junghans and Debashish Mukherji for contributing to the information reported in Sec. IV about the speed up factor.

APPENDIX A: TECHNICAL DETAILS OF THE SIMULATIONS

The potential energy function and the force field parameters for all the molecules were taken from GROMOS53A6 parameter set. Liquid water was described by the SPC model,[21] methanol was described by the model developed by Walser *et al.*,[22] urea by the model described in Ref. 17, tert-butyl alcohol by the parameter set of Ref. 18, and DMSO was described by the model given by Geerke *et al.*[23] For liquid methanol simulations, GROMOS43A1 parameter set was used, as it was shown to be more accurate for calculating excess free energy of solvation of methanol in methanol.[15]

In all the AdResS simulations, the resolution changes only along the x direction. For each system, 30 iterations were performed to obtain a converged thermodynamic force and a flat density profile. Each iteration consisted of 200 ps of equilibration which was followed by 200 ps of data collection. The simulations were performed at *NVT* conditions where the temperature was kept constant at 298 K. Simulations of liquid methane and ethane were performed at 111.66 K and 184.52 K, respectively. As it was discussed in Ref. 5, there is no requirement of a coarse-grained model that resembles the structural and thermodynamic properties of a full atomistic model. It was shown numerically that the proper exchange of

TABLE III. WCA parameters for different coarse-grained molecules used in this work.

System	ϵ (kJ/mol)	σ (nm)
Methane	0.65	0.40
Ethane	0.20	0.50
Propane	0.65	0.55
Methanol	0.65	0.40
DMSO	0.30	0.50
Methanol in methanol/water	0.65	0.40
Methane in methane/water	0.65	0.40
Urea in urea/water	0.65	0.40
Ethane in ethane/water	0.65	0.45
TBA in TBA/water	0.65	0.60
DMSO in DMSO/water	0.65	0.50
TBA in TBA/DMSO	0.40	0.60
DMSO in TBA/DMSO	0.30	0.50

energy and molecules was independent from the molecular model used in the coarse-grained region, showing the convenience of GC-AdResS. In this work, a generic WCA potential was used in the coarse-grained region. The interaction potential between the coarse-grained particles is given by

$$U(r) = 4\epsilon\left[\left(\frac{\sigma}{r}\right)^{12} - \left(\frac{\sigma}{r}\right)^{6}\right] + \epsilon, \quad r \le 2^{1/6}\sigma. \tag{A1}$$

The parameters σ and ϵ were chosen such that the radial distribution functions of particles reproduce a liquid structure. For water molecule, the parameters used in this study are $\epsilon = 0.65$ kJ/mol and $\sigma = 0.30$ nm. Table III shows the WCA parameters for other molecules used in this work. For interactions between solute and solvent, σ values were obtained by averaging over the individual parameters. The solute-solvent ϵ is the same as the solute-solute ϵ.

To obtain the chemical potential of coarse-grained component, insertion particle method was used, where a trajectory of 8 ns was obtained and the coordinates were written after every 0.4 ps. The insertions of the molecule were performed 4 000 000 times in each frame at random locations and with random orientations of the molecule. The excess chemical potential value was calculated by averaging over the last ten iterations after the thermodynamic force has converged and the statistical uncertainty is determined by the standard deviation in the data.

The excess chemical potential of the solute or the excess free energy of solvation was calculated using the TI approach. In the thermodynamic integration, the interaction of solute with the rest of the molecules in the systems is a function of a coupling parameter λ, which indicates a level of change taken place between states A and B. The interactions are switched off as λ is continuously decreased in the stepwise manner. Simulations conducted at different values of λ allow to plot a $\frac{\partial U_i(\lambda)}{\partial \lambda}$ curve, from which μ^{ex} is derived[24]

$$\mu^{\mathrm{ex}}_{iB} - \mu^{\mathrm{ex}}_{iA} = \int_0^1 \left\langle \frac{\partial U_i(\lambda)}{\partial \lambda} \right\rangle_\lambda d\lambda, \tag{A2}$$

where U_i is the interaction energy of particle i with the remaining particles and $\langle \cdot \rangle$ denotes the canonical (*NVT*) or isobaric-isothermal (*NPT*) ensemble average. We computed the excess free energy using a two-stage approach as described in Ref. 25, first coupling van der Waals interactions to transform the non-interacting molecule into a partially interacting uncharged molecule, then coupling Coulomb interactions from an uncharged interacting molecule to fully interacting molecule. The resulting free energy ΔG_{final} is the sum of ΔG values obtained from the two procedures,

$$\Delta G_{final} = \Delta G_{ele} + \Delta G_{vdw}, \tag{A3}$$

where ΔG_{vdw} is the free energy change associated with introducing the van der Waals interactions and ΔG_{ele} is the free energy change associated with introducing Coulomb interactions. We evaluated the above integral for 21 values of λ (evenly spaced between 0 and 1) in both the procedures. At each value of λ, first a steepest descent energy minimization was performed followed by 200 ps of *NPT* equilibration and 400 ps of data collection under constant volume and temperature conditions, in accordance with AdResS simulations. During the van der Waals coupling, soft-core interactions were used with soft-core parameters $\alpha_{LJ} = 0.5$, $\sigma = 0.3$ and the power of λ in soft-core equation was taken as 1. Free energy estimates and the errors were calculated through Bennet's acceptance ratio method (BAR).[26] For both the AdResS and full-atom simulations, the system size was kept same. Table IV gives a detailed summary of each system studied.

In all the simulations, a leap-frog stochastic dynamics integrator with a time step of 2 fs and an inverse friction coefficient of 0.1 ps was used. All bond-lengths were constrained using the LINCS algorithm. For liquid water, methanol, methanol/water, methane/water, and ethane/water, a cut-off radius of 0.9 nm was used for van der Waals and Coulomb interactions, while for rest of the systems, a cut-off radius of 1.4 nm was used. For the TBA/water system, the chemical potential converges at cutoff 0.9 nm for mole-fraction $x_{\mathrm{TBA}} = 0.02$. Since it would be too expensive to do the convergence tests for all concentrations, we simply use a large cutoff 1.4 nm for the concentration dependency study of TBA/water. Electrostatic interactions were calculated using the reaction-field term[27] with a dielectric permittivity of 54 for urea in SPC water,[17] 64.8 for TBA in SPC water,[18] 61 for other solutes in SPC water, 19 for methanol, and 46 for DMSO as the solvent.[15]

APPENDIX B: TECHNICAL ASPECTS OF THE AUXILIARY HAMILTONIAN ADRESS

In principle, when the auxiliary Hamiltonian approach is used, one can perform microcanonical simulations and thus can avoid the use of a thermostat. In this case, the thermodynamic force of the auxiliary Hamiltonian would not carry any effect of the thermostat, and thus the difference between the work of the thermodynamic force of GC-AdResS and that of the auxiliary Hamiltonian is exactly the work that the thermostat does in GC-AdResS in order to compensate energy dissipation. The question is whether the energy is conserved in the auxiliary Hamiltonian approach. We have checked that the conservation holds for systems without electrostatics (methane, ethane, propane), thus for such systems

TABLE IV. Summary of AdResS and full-atom systems.

System	N_{solute}	$N_{solvent}$	System size (nm^3)	AT + HY region (nm^3)
Water	...	13 824	30.2 × 3.8 × 3.8	14.6 × 3.8 × 3.8
Methane	...	2000	9.0 × 3.7 × 3.6	6.0 × 3.7 × 3.6
Ethane	...	2000	12.0 × 3.9 × 3.7	7.0 × 3.9 × 3.7
Propane	...	1433	10.0 × 4.5 × 4.5	7.0 × 4.5 × 4.5
Methanol	...	4000	12.0 × 4.6 × 4.5	7.4 × 4.6 × 4.5
DMSO	...	1500	15.0 × 3.6 × 3.3	7.0 × 3.6 × 3.3
Methanol/water	128	12 672	29.5 × 3.7 × 3.7	14.6 × 3.7 × 3.7
Methane/water	40	6960	10.0 × 4.8 × 4.7	7.0 × 4.8 × 4.7
Urea/water	50	2500	9.7 × 2.9 × 2.8	6.8 × 2.9 × 2.8
Ethane/water	40	6960	10.0 × 4.7 × 4.6	7.0 × 4.7 × 4.6
TBA/water ($x_{\mathrm{TBA}} = 0.001$)	40	39 960	50.1 × 5.8 × 4.3	7.0 × 5.8 × 4.3
TBA/water ($x_{\mathrm{TBA}} = 0.02$)	80	4400	10.0 × 3.6 × 4.2	7.0 × 3.6 × 4.2
TBA/water ($x_{\mathrm{TBA}} = 0.04$)	180	4300	10.0 × 4.3 × 3.7	7.0 × 4.3 × 3.7
TBA/water ($x_{\mathrm{TBA}} = 0.12$)	538	3942	10.0 × 4.4 × 4.6	7.0 × 4.4 × 4.6
TBA/water ($x_{\mathrm{TBA}} = 0.16$)	717	3763	10.0 × 4.9 × 4.6	7.0 × 4.9 × 4.6
TBA/water ($x_{\mathrm{TBA}} = 0.20$)	896	3584	12.0 × 4.6 × 4.5	7.0 × 4.6 × 4.5
DMSO/water	50	4950	12.0 × 4.0 × 3.3	7.0 × 4.0 × 3.3
TBA/DMSO	80	4400	10.0 × 7.3 × 7.2	7.0 × 7.3 × 7.2

the procedure is straightforward. Instead, for systems with electrostatic interactions, even for full atomistic simulations, due to the fact that the force fields are designed for employing the reaction field method, the energy cannot be conserved and the coupling to a thermostat is required. This is a well known problem reported in the manual of Gromacs. However, in our case, for both, the auxiliary Hamiltonian and GC-AdResS the energy drift due to the reaction field method is essentially the same because they have equivalent electrostatic interactions, thus the energy drift due to the use of the reaction field method is automatically removed when we consider the difference between the thermodynamic forces of the two approaches, that is the force of changing resolution.

APPENDIX C: EXTENSION OF THE CHEMICAL POTENTIAL DERIVATION TO MULTI-COMPONENT SYSTEMS

In this section, we extend the chemical potential expression of Eq. (24) to multi-component systems, i.e., we show the derivation (and limitations) of Eq. (25). For simplicity and without lost of generality, we assume that the system is formed by two components A and B, and the number of molecules are N^{A} and N^{B}, respectively. We further denote the number of molecules A in the atomistic, transition, and coarse-grained regions by N_1^{A}, N_2^{A}, and N_3^{A}, respectively, and equivalently for type B, N_1^{B}, N_2^{B}, and N_3^{B}. By assuming, as usual, that the size of the transition region is negligible compared with the atomistic and coarse-grained regions, we have the following constrains:

$$V = V_1 + V_3, \tag{C1}$$

$$N = N^{\mathrm{A}} + N^{\mathrm{B}}, \tag{C2}$$

$$N^{\mathrm{A}} = N_1^{\mathrm{A}} + N_3^{\mathrm{A}}, \tag{C3}$$

$$N^{\mathrm{B}} = N_1^{\mathrm{B}} + N_3^{\mathrm{B}}. \tag{C4}$$

We determine and apply the thermodynamic forces to each component, which are denoted by $\boldsymbol{F}_{\mathrm{th}}^{\mathrm{A}}$ and $\boldsymbol{F}_{\mathrm{th}}^{\mathrm{B}}$; thus, we impose the correct density profile to the system

$$\rho_{\Delta}^{\mathrm{A}} = \rho_{\mathrm{AT}}^{\mathrm{A}} = \rho_{\mathrm{CG}}^{\mathrm{A}} = \rho_0^{\mathrm{A}}, \tag{C5}$$

$$\rho_{\Delta}^{\mathrm{B}} = \rho_{\mathrm{AT}}^{\mathrm{B}} = \rho_{\mathrm{CG}}^{\mathrm{B}} = \rho_0^{\mathrm{B}}. \tag{C6}$$

Similar to Eq. (14), for pure systems, for a mixture in GC-AdResS we have

$$p_{\mathrm{CG}} - p_{\mathrm{AT}} = \rho_0^{\mathrm{A}}\omega_{\mathrm{th}}^{\mathrm{A}} + \rho_0^{\mathrm{B}}\omega_{\mathrm{th}}^{\mathrm{B}}. \tag{C7}$$

Following the same argument of Sec. IV, we have

$$p_{\mathrm{CG}} - p_{\mathrm{AT}} = \rho_0^{\mathrm{A}}\left(\omega_{\mathrm{th}}^{\mathrm{A,H}} - \omega_{\mathrm{rep}}^{\mathrm{A}}\right) + \rho_0^{\mathrm{B}}\left(\omega_{\mathrm{th}}^{\mathrm{B,H}} - \omega_{\mathrm{rep}}^{\mathrm{B}}\right), \tag{C8}$$

where the work of changing representation for molecule A is defined by

$$\omega_{\mathrm{rep}}^{\mathrm{A}} = \omega_{\mathrm{rep}}^{\mathrm{AA}} + \omega_{\mathrm{rep}}^{\mathrm{AB}} = \int_{\Delta} d\boldsymbol{r}\langle \boldsymbol{F}_{\mathrm{rep}}^{\mathrm{AA}}(\boldsymbol{r})\rangle + \int_{\Delta} d\boldsymbol{r}\langle \boldsymbol{F}_{\mathrm{rep}}^{\mathrm{AB}}(\boldsymbol{r})\rangle, \tag{C9}$$

$$\omega_{\mathrm{rep}}^{\mathrm{B}} = \omega_{\mathrm{rep}}^{\mathrm{BA}} + \omega_{\mathrm{rep}}^{\mathrm{BB}} = \int_{\Delta} d\boldsymbol{r}\langle \boldsymbol{F}_{\mathrm{rep}}^{\mathrm{BA}}(\boldsymbol{r})\rangle + \int_{\Delta} d\boldsymbol{r}\langle \boldsymbol{F}_{\mathrm{rep}}^{\mathrm{BB}}(\boldsymbol{r})\rangle, \tag{C10}$$

where $\omega_{\mathrm{rep}}^{\mathrm{AA}}$ denotes the work of changing representation for a molecule of A, due to the interaction with molecules of type A only. Instead, $\omega_{\mathrm{rep}}^{\mathrm{AB}}$ denotes the work of changing representation for a molecule of A, due to the interaction with molecules of type B only. The same terminology holds for $\omega_{\mathrm{rep}}^{\mathrm{BA}}$ and $\omega_{\mathrm{rep}}^{\mathrm{BB}}$.

The explicit expressions are

$$\langle \boldsymbol{F}^{\mathrm{AA}}_{\mathrm{rep}}(\boldsymbol{r})\rangle = \nabla_{\boldsymbol{r}} w(\boldsymbol{r})\Big\langle w(\boldsymbol{r}')\Big[\sum_{\alpha,\beta} U^{\mathrm{AT}}_{\mathrm{AA}}(\boldsymbol{r}_\alpha - \boldsymbol{r}'_\beta) - U^{\mathrm{CG}}_{\mathrm{AA}}(\boldsymbol{r}-\boldsymbol{r}')\Big]\Big\rangle_{\boldsymbol{r}',\mathrm{A};\boldsymbol{r},\mathrm{A}}, \tag{C11}$$

$$\langle \boldsymbol{F}^{\mathrm{AB}}_{\mathrm{rep}}(\boldsymbol{r})\rangle = \nabla_{\boldsymbol{r}} w(\boldsymbol{r})\Big\langle w(\boldsymbol{r}')\Big[\sum_{\alpha,\beta} U^{\mathrm{AT}}_{\mathrm{AB}}(\boldsymbol{r}_\alpha - \boldsymbol{r}'_\beta) - U^{\mathrm{CG}}_{\mathrm{AB}}(\boldsymbol{r}-\boldsymbol{r}')\Big]\Big\rangle_{\boldsymbol{r}',\mathrm{B};\boldsymbol{r},\mathrm{A}}, \tag{C12}$$

$$\langle \boldsymbol{F}^{\mathrm{BA}}_{\mathrm{rep}}(\boldsymbol{r})\rangle = \nabla_{\boldsymbol{r}} w(\boldsymbol{r})\Big\langle w(\boldsymbol{r}')\Big[\sum_{\alpha,\beta} U^{\mathrm{AT}}_{\mathrm{BA}}(\boldsymbol{r}_\alpha - \boldsymbol{r}'_\beta) - U^{\mathrm{CG}}_{\mathrm{BA}}(\boldsymbol{r}-\boldsymbol{r}')\Big]\Big\rangle_{\boldsymbol{r}',\mathrm{A};\boldsymbol{r},\mathrm{B}}, \tag{C13}$$

$$\langle \boldsymbol{F}^{\mathrm{BB}}_{\mathrm{rep}}(\boldsymbol{r})\rangle = \nabla_{\boldsymbol{r}} w(\boldsymbol{r})\Big\langle w(\boldsymbol{r}')\Big[\sum_{\alpha,\beta} U^{\mathrm{AT}}_{\mathrm{BB}}(\boldsymbol{r}_\alpha - \boldsymbol{r}'_\beta) - U^{\mathrm{CG}}_{\mathrm{BB}}(\boldsymbol{r}-\boldsymbol{r}')\Big]\Big\rangle_{\boldsymbol{r}',\mathrm{B};\boldsymbol{r},\mathrm{B}}. \tag{C14}$$

The notations are self-explanatory; for example, $U^{\mathrm{AT}}_{\mathrm{AB}}$ denotes the expression for atomistic interactions between one molecule of type A and one of type B ($U^{\mathrm{AT}}_{\mathrm{AA}}$ and$U^{\mathrm{AT}}_{\mathrm{BB}}$ are similar), while $U^{\mathrm{CG}}_{\mathrm{AB}}$ is the equivalent for coarse-grained interactions. Notation $\langle\cdot\rangle_{\boldsymbol{r}',\mathrm{B};\boldsymbol{r},\mathrm{A}}$ denotes the ensemble average performed with respect to position $\boldsymbol{r}'$ of molecule B, provided that a molecule A takes the position $\boldsymbol{r}$ (the same applies for other combinations on indices $\boldsymbol{r}'$, $\boldsymbol{r}$, A, B). If molecules contain more than one atom, then the average is also taken over all possible conformations. Therefore, the physical meaning of (for example) force $\langle \boldsymbol{F}^{\mathrm{AB}}_{\mathrm{rep}}(\boldsymbol{r})\rangle$ is that of an average force at $\boldsymbol{r}$ acting on a molecule of type A due to the interaction with molecules of type B. Although we have $U^{\mathrm{AT}}_{\mathrm{AB}} = U^{\mathrm{AT}}_{\mathrm{BA}}$ and $U^{\mathrm{CG}}_{\mathrm{AB}} = U^{\mathrm{CG}}_{\mathrm{BA}}$, it should be noted that we do not have $\omega^{\mathrm{BA}}_{\mathrm{rep}} = \omega^{\mathrm{AB}}_{\mathrm{rep}}$ in general. From Eqs. (C7)–(C10), we have

$$\rho^{\mathrm{A}}_0\left(\omega^{\mathrm{A,H}}_{\mathrm{th}} - \omega^{\mathrm{A}}_{\mathrm{th}} - \omega^{\mathrm{AA}}_{\mathrm{rep}} - \omega^{\mathrm{AB}}_{\mathrm{rep}}\right) + \rho^{\mathrm{B}}_0\left(\omega^{\mathrm{B,H}}_{\mathrm{th}} - \omega^{\mathrm{B}}_{\mathrm{th}} - \omega^{\mathrm{BA}}_{\mathrm{rep}} - \omega^{\mathrm{BB}}_{\mathrm{rep}}\right) = 0. \tag{C15}$$

We denote the work done in the transition region on the two types of molecules by ω^{A}_0 and ω^{B}_0, respectively. The chemical potential difference between the AT and CG resolution, can be derived following the same procedure presented in Sec. III.C of Ref. 5 which can be extended to the two component system in a straightforward way. Such a procedure leads to

$$\mu^{\mathrm{A}}_{\mathrm{AT}}\left(N^{\mathrm{A}}_1, N^{\mathrm{B}}_1, V_1, T\right) = \mu^{\mathrm{A}}_{\mathrm{CG}}\left(N^{\mathrm{A}}_3, N^{\mathrm{B}}_3, V_3, T\right) - \omega^{\mathrm{A}}_0, \tag{C16}$$

$$\mu^{\mathrm{B}}_{\mathrm{AT}}\left(N^{\mathrm{A}}_1, N^{\mathrm{B}}_1, V_1, T\right) = \mu^{\mathrm{B}}_{\mathrm{CG}}\left(N^{\mathrm{A}}_3, N^{\mathrm{B}}_3, V_3, T\right) - \omega^{\mathrm{B}}_0. \tag{C17}$$

In the thermodynamic limit, these numbers maximize the Helmholtz free energy. In this context, the chemical potential, e.g., $\mu^{\mathrm{A}}_{\mathrm{AT}}$, is the free energy increment due to the insertion of one molecule of type A into the infinitely large A–B mixture.

Similar to the case of the one component system, from Eqs. (C16) and (C17), we write down for GC-AdResS

$$\mu^{\mathrm{A}}_{\mathrm{CG}} - \mu^{\mathrm{A}}_{\mathrm{AT}} = \omega^{\mathrm{A}}_{\mathrm{th}} + \omega^{\mathrm{A}}_{\mathrm{DOF}} + \omega^{\mathrm{A}}_{\mathrm{extra}}, \tag{C18}$$

$$\mu^{\mathrm{B}}_{\mathrm{CG}} - \mu^{\mathrm{B}}_{\mathrm{AT}} = \omega^{\mathrm{B}}_{\mathrm{th}} + \omega^{\mathrm{B}}_{\mathrm{DOF}} + \omega^{\mathrm{B}}_{\mathrm{extra}}. \tag{C19}$$

$\omega^{\mathrm{A}}_{\mathrm{th}}$ and $\omega^{\mathrm{B}}_{\mathrm{th}}$ are the work of the thermodynamic force $\boldsymbol{F}^{\mathrm{A}}_{\mathrm{th}}$ and $\boldsymbol{F}^{\mathrm{B}}_{\mathrm{th}}$, respectively. $\omega^{\mathrm{A}}_{\mathrm{extra}}$ is the energy dissipation due to molecule A that changes resolution in the transition region, and $\omega^{\mathrm{B}}_{\mathrm{extra}}$ is defined similarly. The energy dissipation can be further divided as

$$\omega^{\mathrm{A}}_{\mathrm{extra}} = \omega^{\mathrm{AA}}_{\mathrm{extra}} + \omega^{\mathrm{AB}}_{\mathrm{extra}}, \tag{C20}$$

$$\omega^{\mathrm{B}}_{\mathrm{extra}} = \omega^{\mathrm{BA}}_{\mathrm{extra}} + \omega^{\mathrm{BB}}_{\mathrm{extra}}. \tag{C21}$$

$\omega^{\mathrm{AA}}_{\mathrm{extra}}$ is the energy dissipation of a molecule A produced by non-conservative interactions between molecule type A and type A only. Similarly, $\omega^{\mathrm{AB}}_{\mathrm{extra}}$ is the energy dissipation of a molecule A due to the non-conservative interactions with molecules of type B. The definitions are similar for $\omega^{\mathrm{BA}}_{\mathrm{extra}}$ and $\omega^{\mathrm{BB}}_{\mathrm{extra}}$. It should be noticed that, we do not have $\omega^{\mathrm{BA}}_{\mathrm{extra}} = \omega^{\mathrm{AB}}_{\mathrm{extra}}$ in general. For the expression of the chemical potential, the same argument as above, is applied to the auxiliary Hamiltonian approach, and yields

$$\mu^{\mathrm{A}}_{\mathrm{CG}} - \mu^{\mathrm{A}}_{\mathrm{AT}} = \omega^{\mathrm{A,H}}_{\mathrm{th}} + \omega^{\mathrm{A}}_{\mathrm{DOF}}, \tag{C22}$$

$$\mu^{\mathrm{B}}_{\mathrm{CG}} - \mu^{\mathrm{B}}_{\mathrm{AT}} = \omega^{\mathrm{B,H}}_{\mathrm{th}} + \omega^{\mathrm{B}}_{\mathrm{DOF}}. \tag{C23}$$

By using Eqs. (C18), (C20), and (C22) we have

$$\omega^{\mathrm{AA}}_{\mathrm{extra}} + \omega^{\mathrm{AB}}_{\mathrm{extra}} = \omega^{\mathrm{A,H}}_{\mathrm{th}} - \omega^{\mathrm{A}}_{\mathrm{th}}. \tag{C24}$$

Using Eqs. (C19), (C21), and (C23) we have

$$\omega^{\mathrm{BA}}_{\mathrm{extra}} + \omega^{\mathrm{BB}}_{\mathrm{extra}} = \omega^{\mathrm{B,H}}_{\mathrm{th}} - \omega^{\mathrm{B}}_{\mathrm{th}}. \tag{C25}$$

By inserting Eqs. (C24) and (C25) into Eq. (C15), we have

$$\rho^{\mathrm{A}}_0\left(\omega^{\mathrm{AA}}_{\mathrm{extra}} + \omega^{\mathrm{AB}}_{\mathrm{extra}} - \omega^{\mathrm{AA}}_{\mathrm{rep}} - \omega^{\mathrm{AB}}_{\mathrm{rep}}\right) + \rho^{\mathrm{B}}_0\left(\omega^{\mathrm{BA}}_{\mathrm{extra}} + \omega^{\mathrm{BB}}_{\mathrm{extra}} - \omega^{\mathrm{BA}}_{\mathrm{rep}} - \omega^{\mathrm{BB}}_{\mathrm{rep}}\right) = 0. \tag{C26}$$

It is natural to conclude that $\omega^{\mathrm{AA}}_{\mathrm{extra}} = \omega^{\mathrm{AA}}_{\mathrm{rep}}$, because these two terms exclusively involve A–A interaction. The same is true for B–B interaction: $\omega^{\mathrm{BB}}_{\mathrm{extra}} = \omega^{\mathrm{BB}}_{\mathrm{rep}}$. The physical meaning of $\omega^{\mathrm{AB}}_{\mathrm{extra}}$, $\omega^{\mathrm{AB}}_{\mathrm{rep}}$, $\omega^{\mathrm{BA}}_{\mathrm{extra}}$ and $\omega^{\mathrm{BA}}_{\mathrm{rep}}$, leads to identify of $\omega^{\mathrm{AB}}_{\mathrm{extra}}$ with $\omega^{\mathrm{AB}}_{\mathrm{rep}}$, and $\omega^{\mathrm{BA}}_{\mathrm{extra}}$ with $\omega^{\mathrm{BA}}_{\mathrm{rep}}$. It follows that (for example) for component A, the excess chemical potential difference is

$$\mu^{\mathrm{A,ex}}_{\mathrm{CG}} - \mu^{\mathrm{A,ex}}_{\mathrm{AT}} = \int_\Delta \boldsymbol{F}^{\mathrm{A}}_{\mathrm{th}}(\boldsymbol{r})d\boldsymbol{r} + \int_\Delta \langle \boldsymbol{F}^{\mathrm{AA}}_{\mathrm{rep}}(\boldsymbol{r})\rangle d\boldsymbol{r} + \int_\Delta \langle \boldsymbol{F}^{\mathrm{AB}}_{\mathrm{rep}}(\boldsymbol{r})\rangle d\boldsymbol{r}, \tag{C27}$$

and this proves Eq. (25).

[1]B. Widom, J. Chem. Phys. **39**, 2808 (1963).
[2]I. G. Tironi and W. F. van Gunsteren, Mol. Phys. **83**, 381 (1994).
[3]S. Fritsch, S. Poblete, C. Junghans, G. Ciccotti, L. Delle Site, and K. Kremer, Phys. Rev. Lett. **108**, 170602 (2012).
[4]H. Wang, C. Schütte, and L. Delle Site, J. Chem. Theory Comput. **8**, 2878 (2012).

[5]H. Wang, C. Hartmann, C. Schütte, and L. Delle Site, Phys. Rev. X **3**, 011018 (2013).
[6]J. Zavadlav, M. N. Melo, S. J. Marrink, and M. Praprotnik, J. Chem. Phys. **140**, 054114 (2014).
[7]J. Zavadlav, M. N. Melo, A. Vicente Cunha, A. H. De Vries, S. J. Marrink, and M. Praprotnik, J. Chem. Theory Comput. **10**, 2591–2598 (2014).
[8]R. Potestio, S. Fritsch, P. Espanol, R. Delgado-Buscalioni, K. Kremer, R. Everaers, and D. Donadio, Phys. Rev. Lett. **111**, 060601 (2013).
[9]R. Potestio, S. Fritsch, P. Espanol, R. Delgado-Buscalioni, K. Kremer, R. Everaers, and D. Donadio, Phys. Rev. Lett. **110**, 108301 (2013).
[10]L. Delle Site, Entropy **16**, 23–40 (2014).
[11]C. Junghans and S. Poblete, Comput. Phys. Commun. **181**, 1449 (2010).
[12]D. Mukherji, N. F. A. van der Vegt, and K. Kremer, J. Chem. Theory Comput. **8**, 3536 (2012).
[13]K. Yoshida, T. Yamaguchi, A. Kovalenko, and F. Hirata, J. Phys. Chem. B **106**, 5042 (2002).
[14]H. Eslami and F. Müller-Plathe, J. Comput. Chem. **28**, 1763 (2007).
[15]D. P. Geerke and W. F. van Gunsteren, ChemPhysChem **7**, 671 (2006).
[16]J. R. Pliego, Jr. and J. M. Riveros, Phys. Chem. Chem. Phys. **4**, 1622 (2002).
[17]L. J. Smith, H. J. C. Berendsen, and W. F. van Gunsteren, J. Phys. Chem. B **108**, 1065 (2004).
[18]M. E. Lee and N. F. A. van der Vegt, J. Chem. Phys. **122**, 114509 (2005).
[19]D. Mukherji, N. F. A. van der Vegt, K. Kremer, and L. Delle Site, J. Chem. Theory Comput. **8**, 375 (2012).
[20]See http://www.gromacs.org/ for more information about the GROMACS code.
[21]H. J. C. Berendsen, J. P. M. Postma, W. F. van Gunsteren, and J. Hermans, "Interaction models for water in relation to protein hydration," in *Intermolecular Forces*, edited by B. Pullman (Reidel, Dordrecht, 1981), p. 331.
[22]R. Walser, A. E. Mark, W. F. van Gunsteren, M. Lauterbach, and G. Wipff, J. Chem. Phys. **112**, 10450 (2000).
[23]D. P. Geerke, C. Oostenbrink, N. F. A. van der Vegt, and W. F. van Gunsteren, J. Phys. Chem. B. **108**, 1436 (2004).
[24]T. Kristof and G. Rutkai, Chem. Phys. Lett. **445**, 74 (2007).
[25]D. L. Mobley, J. D. Chodera, and K. A. Dill, J. Chem. Phys. **125**, 084902 (2006).
[26]C. H. Bennett, J. Comput. Phys. **22**, 245 (1976).
[27]I. G. Tironi, R. Sperb, P. E. Smith, and W. F. van Gunsteren, J. Chem. Phys. **102**, 5451 (1995).